CHAPTER 7

Microbial Removal of Cr (VI), Pb (II) and Cd (II) by a New Bacterial Strain Isolated from the Site Contaminated with Coal Mine Effluents

Chapter 7: Microbial Removal of Cr (VI), Pb (II) and Cd (II) by a New Bacterial Strain Isolated from the Site Contaminated with Coal Mine Effluents

7.1 Introduction

Heavy metal ions such as Cr (VI), Cd (II) and Pb (II) are used in several industrial applications such as pigment and paint manufacturing, glass and batteries built-up and chrome plating [Sarangi et al., 2008]. The effluent emanating from these industrial units adds a large amount of heavy metal ions in the aquatic and terrestrial ecosystems [Singh et al. 2021a; Singh et al., 2020]. The exposure of heavy metal ions occurs through intake of contaminated water, food or contact with skin and results in several types of cancers, nephrological and neurological disorders [Balali-Mood et al., 2021]. Therefore, removal of heavy metal ions from the wastewater is needful for the environment and human beings [Garg et al., 2012]. The conventional methods of heavy metal removal such as ion-exchange, hydroxide precipitation, osmosis, reverse osmosis, electro-coagulation and flocculation, membrane filtration and adsorption [Singh et al. 2021b] have been extensively practised in past. However, these methods have some disadvantages like incomplete heavy metal removal from liquid phase, high operational cost and production of secondary chemical sludge at the end of the process [Goksungur et al., 2005]. Hence, it is needful to find out suitable heavy metal removal method for treatment of wastewater [Singh et al. 2020]. Promising and effective results in terms of heavy metal removal have been obtained by using living biomass as a bio-remediating agent [Elahi et al., 2020]. The benefits of using a living biomass for removal of heavy metal are its inexpensiveness, generation of a small amount of secondary biological sludge at the end, simple treatment methodology, no requirement of skilled work and effective in removing heavy metals from a very low concentration [Hedayatkhah et al., 2018]. Among the living biomass systems, the bacteria have a prodigious heavy metal resistance and bio-accumulate metal ions

within their intracellular space through their cell surface receptors [Jacob et al., 2018]. Various bacterial genera such as *Pseudomonas* [El-Naggar et al., 2020], *Klebsiella* [Tekerlekopoulou et al., 2013], *Microbacterium* [Humphries et al., 2005] and *Bacillus* [Li et al., 2020b], which are highly heavy metal resistant have been isolated in the scientific literature. Additionally, bioremediation mediated by bacteria is considered as an eco-friendly and inexpensive method [Ibrahim et al., 2012].

Bacterial strain isolated in the heavy metal contaminated sites are highly resistant to the heavy metal ions [Liu et al., 2012]. The antioxidant system in the bacteria reduces the heavy metal toxicity [Garg et al., 2013]. ROS is generated in the bacterial cell due to metal toxicity [Kubrak et al., 2010]. ROS are highly reactive species and have lethal effects on the bacterial cell. The antioxidant enzymes expressed in the heavy metal stress, capture ROS species and reduce metal toxicity [Kumar et al., 2013]. Thus, antioxidant activity of bacterial cells actively participates in the detoxification and bioremediation of heavy metal ions [Joutey et al., 2015].

The present work aims at isolation, identification and characterization of heavy metal resistant-cum-bioremediating bacteria from the location contaminated with coal mine effluents (Baliya Nala, Singrauli, Madhya Pradesh, India). The bacterial isolate was identified by 16S rRNA gene sequencing. Besides this, bacterial growth and morphological changes were studied against several Cr (VI), Cd (II) and Pb (II) concentrations. ANN study was conducted to predict optimum conditions for the removal of heavy metal ions. The heavy metal removal potential of the bacterial isolate was also examined at different intervals of time. The contrivance of bacterial mediated bioremediation was investigated in the term of antioxidant production and dimensionless numbers were used to describe mechanism of heavy metal removal.

7.2.0 Physico-chemical characterization of wastewater (Source of water collection: Baliya Nala, Singrauli, Madhya Pradesh, India)

The physicochemical characterization of wastewater is shown in Table 7.1 and is compared with the permissible discharge limit of industrial effluent as demarcated by CPCB, India.

Table 7.1 Physico-chemical characterization of wastewater

Physicochemical parameters	**Wastewater**	**CPCB (2000)**
pH	4.90 ± 0.30	5.50-9.00
Temperature (ºC)	36.50 ± 0.32	20.00-30.00
Suspended solids (mg/L)	636.00 ± 1.52	100.00
Phosphate (mg/L)	37.02 ± 2.09	5.00
Ammonia (mg/L)	54.08 ± 1.91	5.00
Nitrate (mg/L)	31.02 ± 2.15	10.00-50.00
DO (mg/L)	1.92 ± 0.31	3.00-5.00
BOD (mg/L)	34.23 ± 1.31	30.00-150.00
Cr (mg/L)	4.02 ± 0.32	1.00-2.00
Ni (mg/L)	5.68 ± 0.12	2.00-3.00
Pb (mg/L)	12.02 ± 0.23	0.10
As (mg/L)	0.89 ± 0.08	0.20
Cd (mg/L)	21.09 ± 0.83	0.20-2.00
Zn (mg/L)	6.12 ± 0.41	5.00

Wastewater characterization showed that it was highly polluted with Cr, Ni, Pb, As, Cd and Zn. The pH of wastewater was slightly acidic, which is harmful to aquatic animals. The level of suspended particles in the wastewater was greater than the permissible discharge limit. These pollutants degrade the water quality. The suspended solid particles hinder the flow of water and is also unsuitable for breeding aquatic animals [Ghose et al., 2001]. Ammonia,

phosphate and BOD values were remarkably high in the wastewater. The dissolved oxygen concentration was much lower, which indicated a significant pollution level [Kapse et al., 2017].

7.3.0 Characterization of bacterial isolate

7.3.1 16S rRNA gene sequencing

The presence of 16S rRNA gene product was confirmed through gel electrophoresis and imaging in a gel documentation system (Figure 7.1).

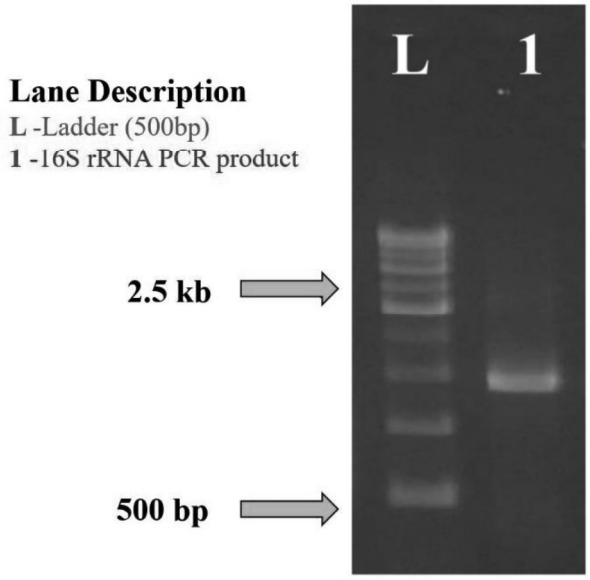

Figure 7.1 Gel electrophoresis image of amplified 16S rRNA gene of isolated bacteria

Gel image showed the presence and size of amplified 16S rRNA gene. The lane L represents the DNA marker (ladder) of 500 bp. 16S gene product in lane 1 is amplified 16S gene. Gel electrophoresis image showed that band size in lane 1 was between 1200-1600 bp, which confirmed the successful amplication of 16S rRNA gene in the PCR reaction [dos Santos et al., 2019]. Figure 7.2 represents the evolutionary relationship among bacterial isolate and reference sequences available in the NCBI database.

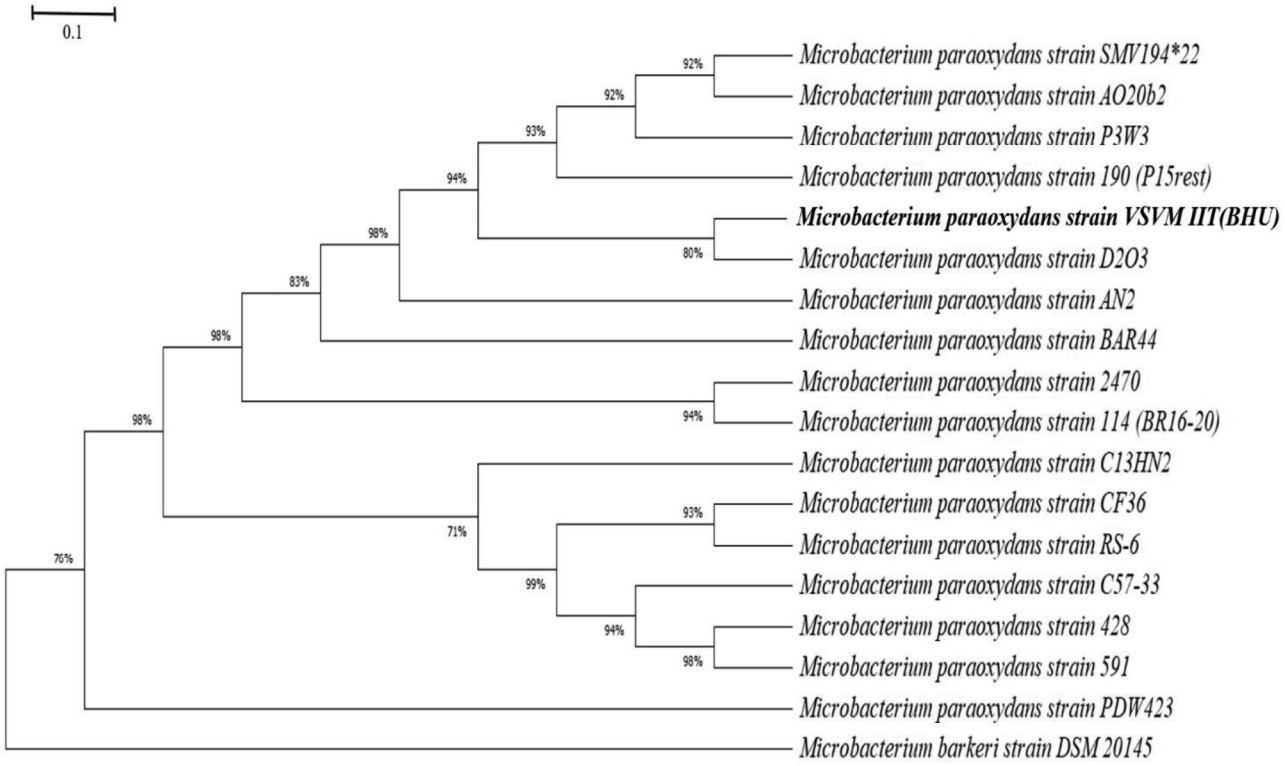

Figure 7.2 Phylogenetic tree of *Microbacterium paraoxydans* strain VSVM IIT (BHU) (accession number (MN650647). The analysis includes 18 nucleotide sequence.

The bacterial isolate showed maximum similarity with *Microbacterium paraoxydans.* Gene sequence of *Microbacterium paraoxydans* strain VSVM IIT(BHU) was submitted to the NCBI GenBank database and accession number MN650647 was obtained.

The evolutionary analysis of bacterial isolate *Microbacterium paraoxydans* strain VSVM IIT(BHU) showed its closed evolutionary relationship with *Microbacterium paraoxydans* strain D2O3. *Microbacterium paraoxydans* strain VSVM IIT (BHU) showed grouping with other strains of *Microbacterium paraoxydans*. An external strain *Microbacterial barkeri* strain DSM 20145 confirmed this grouping, being located outside of the entire tree.

Fan et al., 2018 isolated toxic metal resistant bacteria from the root of *Rohbina pseudocacia* grown in the mining area. Authors performed 16S rRNA gene sequencing and phylogenetic tree was constructed by using MEGA X software. The 16S rRNA gene

sequencing method is much advantageous and accurate in comparison to other biochemical characterization techniques. Xiao et al., 2017 used similar approach for identifying Cr (VI) tolerant bacteria isolated from electroplating industrial sludge. Gupta et al., 2018 identified chromium reducing bacteria *Klebsiella* sp. by using gene sequencing approach. Bharagava and Mishra, 2018 isolated Cr (VI) resistant bacteria from the leather industry effluent and identified as *Cellulosimicrobium* sp. by using gene sequencing method. Kaushik et al., 2012 isolated four bacterial species from the soil contaminated with textile effluent and identified them through 16S rRNA gene sequencing. The author reported that bacterial isolates showed a close evolutionary relationship with *Microbacterium paraoxydans* and bacterial isolates were identified as *Microbacterium paraoxydans* strain 3109 and *Microbacterium paraoxydans* strain CF36. The other two bacterial isolates showed similarity with *Microbacterium* sp. CQ0110Y, *Microbacterium* sp. GE1017. Waranusantigul et al., 2011 isolated lead tolerant bacteria (*Microbacterium paraoxydans* BN-2) and reported close similarity with *Microbacterium paraoxydans*. Benmalek and Fardeau, 2016 isolated multi heavy metal resistant bacteria from wastewater. Authors performed 16S rRNA gene sequence and phylogenetic analysis of bacterial isolate and identified it as *Micrococcus* sp. strain 2YB-25OH. Raja et al., 2006 isolated Ni (II), Pb (II), Cd (II) and Cr (VI) resistant bacteria from oil mill industry effluent. The bacterial isolates were characterized by16S rRNA gene sequencing followed by BLAST and phylogenetic analysis, and bacterial isolated was reported as *Pseudomonas aeruginosa* and *Pseudomonas* BC15.

7.3.2 SEM and EDX analysis

The SEM of *Microbacterium paraoxydans* strain VSVM IIT(BHU) exposed to Cr (VI), Cd (II), Pb (II) in single and ternary metal ion system is shown in Figure 7.3

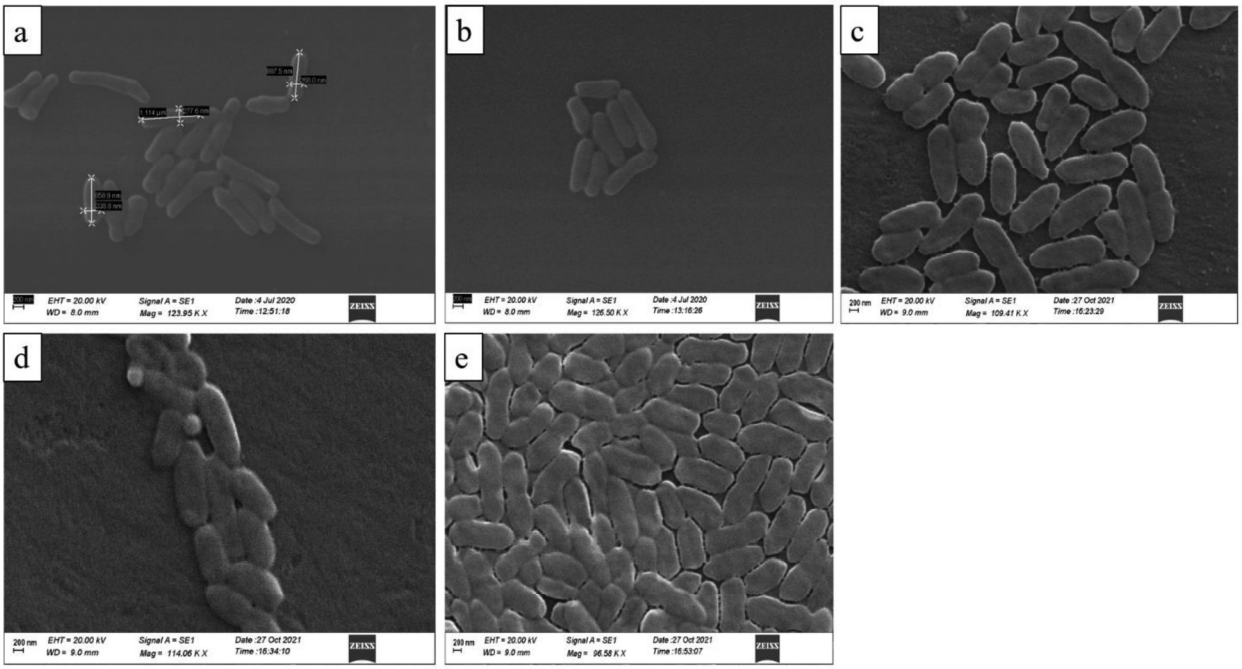

Figure 7.3 SEM of bacterial isolate of control (a), Cr (VI) (b), Cd (II) (c), Pb (II) (d) exposed in single and exposed in ternary metal ion system.

The results of SEM analysis indicated that the bacterial isolate was elongated, rod shaped, uniform and smooth surface. The bacterial cells were 953.46 long and 294.8 nm wide. However, as soon as bacterial isolate was exposed to Cr (VI) (Figure 7.3b), Cd (II) (Figure 7.3c), Pb (II) (Figure 7.3d) in single and ternary (Figure 7.3e) metal ion system, the roughness of bacterial surface increased as compared to the control (Figure 7.3a). The cell roughness after heavy metal exposure was might be due to the deposition of sticky secretion on the bacterial cell surface [Das et al., 2013]. Zhang and Li, 2011 found similar surface modifications in *Serratia* sp. Cr-10 grown in Cr (VI). Pei et al., 2009 investigated the Cr (VI) removal efficiency of *Acinetobactor haemolyticus*. They observed that the surface of microorganism became rough after growing it in the growth medium spiked with Cr (VI). Sodhi et al., 2020 investigated heavy metal removal using *Alcaligenes* sp. MMA and also analysed surface morphology using SEM. Authors reported that the roughness of bacterial surface was increased after bacterial cells exposed with Cd (II). Shao et al., 2019 investigated *Bacillus* sp. cells

morphology changes after exposure of Pb (II) and Cr (VI). Authors observed that cell surface became rough and shape of cells were also changed due to heavy metal toxicity.

Mishra et al., 2021 isolated *Microbacterium paraoxydans* strain from tannery effluent and investigated Cr (VI) reduction using bacterial isolate. Authors also investigated SEM analysis of bacteria isolated found elongated and rod shaped bacterial strain. Reis-Mansur et al., 2019 isolated *Microbacterium* sp. LEMMJ01 from Antarctic soil. Authors investigated morphology of bacterial isolate under SEM and reported elongated and rod shaped bacterial structure. Gua et al., 2013 isolated *Microbacterium neimengense sp.* from rhizosphere of maize. Authors reported similar kind of bacterial shape and morphology in the SEM analysis.

EXD analysis confirmed the presence of elements which are the component of bacterial cell and indicated towards biosorption of heavy metal ions on the bacterial surface. The EDX analysis of control and heavy metal exposed bacterial isolate is shown in Figure 7.4.

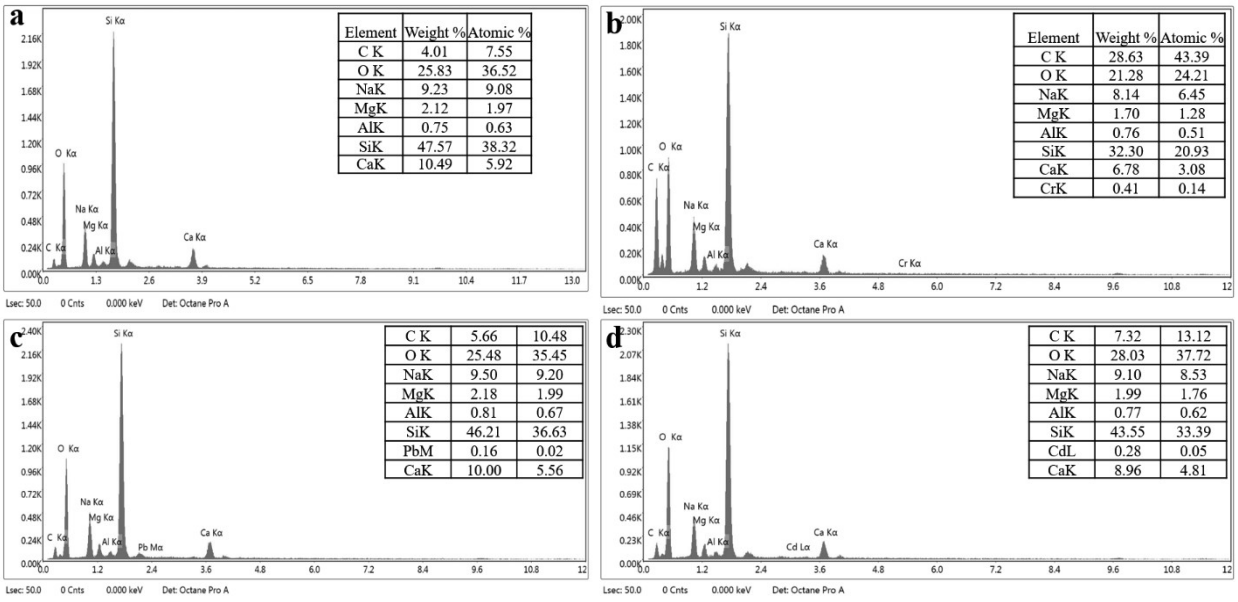

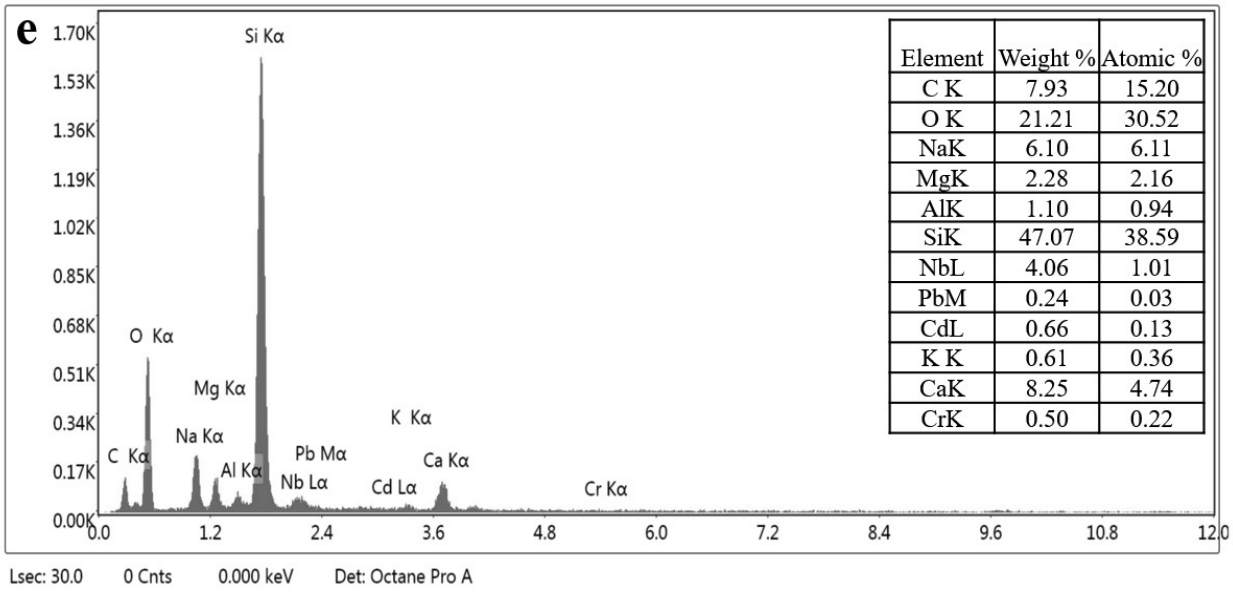

Element	Weight %	Atomic %
C K	7.93	15.20
O K	21.21	30.52
NaK	6.10	6.11
MgK	2.28	2.16
AlK	1.10	0.94
SiK	47.07	38.59
NbL	4.06	1.01
PbM	0.24	0.03
CdL	0.66	0.13
K K	0.61	0.36
CaK	8.25	4.74
CrK	0.50	0.22

Figure 7.4 EDX analysis of control **(a),** and Cr (VI) **(b),** Pb (II) **(c),** Cd (II) **(d)** and ternary metal ion **(e)** exposed *Microbacterium paraoxydans* strain VSVM IIT(BHU)

The EDX analysis suggested that C, O, Na, Mg, Al, Si and Ca were present on control (Figure 7.4a) and heavy metal exposed (Figure 7.4b-e) bacterial surfaces. The EDX indicated that the Si, C and O were major elements on *Microbacterium paraoxydans* strain VSVM IIT(BHU) surface. These elements provide active binding sites in ample number for the biosorption of heavy metals [Singh et al., 2020]. The presence of carbon makes the *Microbacterium paraoxydans* strain VSVM IIT(BHU) suitable for the adsorption of heavy metal ions from wastewater [Labied et al., 2018]. The surface silica has a strong binding affinity for heavy metal ions, which is mediated through the complex formation [Oh et al., 2007]. Both silica and oxygen are responsible for mesoporous amorphous structure, which is suitable for the heavy metal adsorption on the bacterial surface [Bois et al., 2003]. Cr (VI), Cd (II) and Pd (II) also appreared on the surface of *Microbacterium paraoxydans* strain VSVM IIT(BHU) in the bacterial cells grown in medium spiked with single (Figure 7.4 b-d) and ternary (Figure 7.4 e) metal heavy ion system. The presence of heavy metal ions on the bacterial surface confirmed the biosorption of Cr (VI), Cd (II) and Pb (II) by bacteria. Das et al., 2013 investigated Cr (VI)

removal by *B. amyloliquefaciens* and also performed SEM-EDX analysis of bacterial isolate before and after Cr (VI) removal. Authors also reported presence of Cr (VI) on the bacterial surface after Cr (VI) biosorption. Zeng et al., 2019 isolated Cr (VI) resistant bacteria from contaminated soil. Authors reported that bacterial cell surface provides a suitable environment for the Cr (VI) reduction and suface fuctional groups played an important role in its detoxification. Syed and Chinthala, 2015 investigated Cu (II), Pb (II) and Cd (II) bioremediation by using *Bacillus* sp. isolated from Solar Salterns. Authors performed EDX analysis for heavy metal exposed bacterial species and reported successful biosorption of Cd (II), Pb (II) and Cu (II) on the cell of bacterial cells. Goswami et al., 2017 investigated bioremediation of Cd (II), Ni (II), Pb (II), Cu (II), Zn (II) and Fe (II) by *Rhodococcus opacus* bacteria. Authors also performed SEM-EDX analysis of heavy metal exposed *Rhodococcus opacus* and reported biosorption of heavy metal ions on the bacterial cells. Shamim et al., 2013 investigated Pb (II) removal by *Aeromonas caviae* strain KS-1. In the EXD analysis authors observed binding of Pb (II) to the bacterial cells which indicated the efficacious biosorption of Pb (II) by bacteria.

7.3.3 XPS analysis

The XPS analysis was performed to confirm presence of heavy metal ions in the bacterial cell. XPS analysis also confirmed the presence of elemental components in the bacterial cells. The XPS analysis of control and *Microbacterium paraoxydans* strain VSVM IIT(BHU) exposed to heavy metal ions are shown in the Figure 7.5.

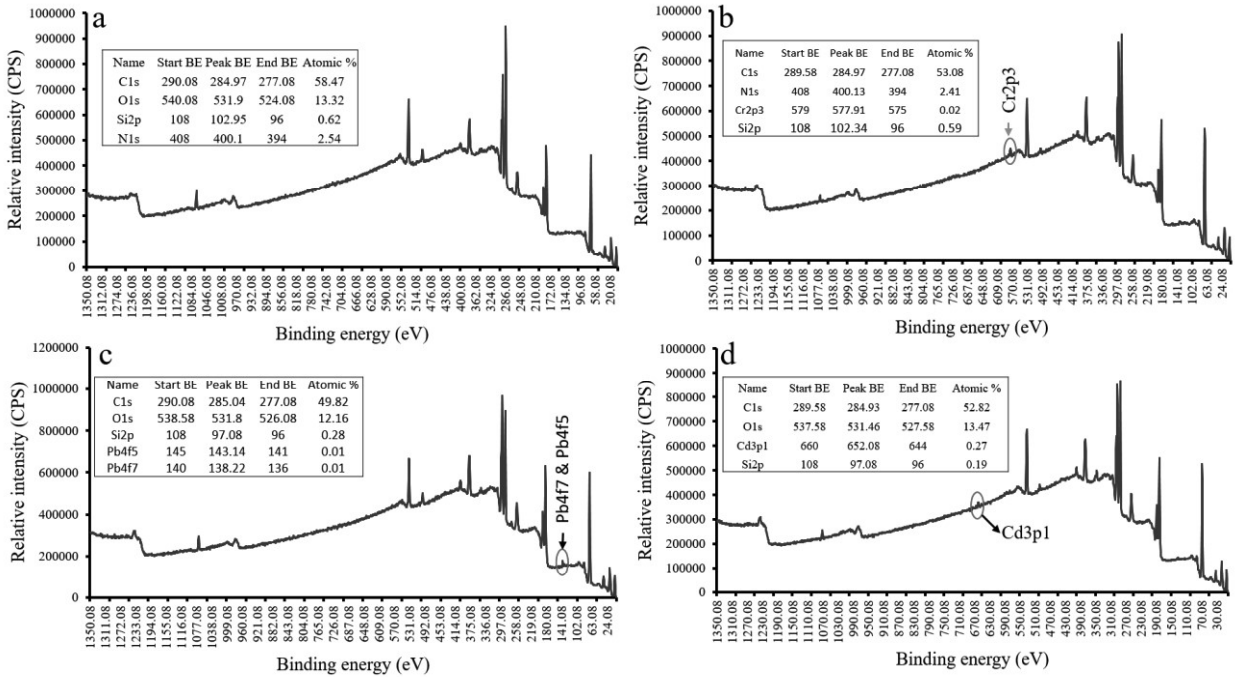

Figure 7.5 XPS analysis of control (**a**), Cr (VI) (**b**), Pb (II) (**c**) and Cd (II) (**d**) exposed *Microbacterium paraoxydans* strain VSVM IIT(BHU)

The C and O elements were present on the bacterial cell in majority as these elements are the major component of living cells (Figure 7.5a). The N and Si were observed in the XPS analysis in the bacterial cells. The XPS analysis clearly indicated that Cr (VI), Pb (II) and Cd (II) ions bonded with bacterial cells (Figure 7.5 b-d). The simultaneous removal of Cr (VI), Pb (II) and Cd (II) was also conducted and XPS of heavy metal ions exposed bacterial cells is shown in Figure 7.6.

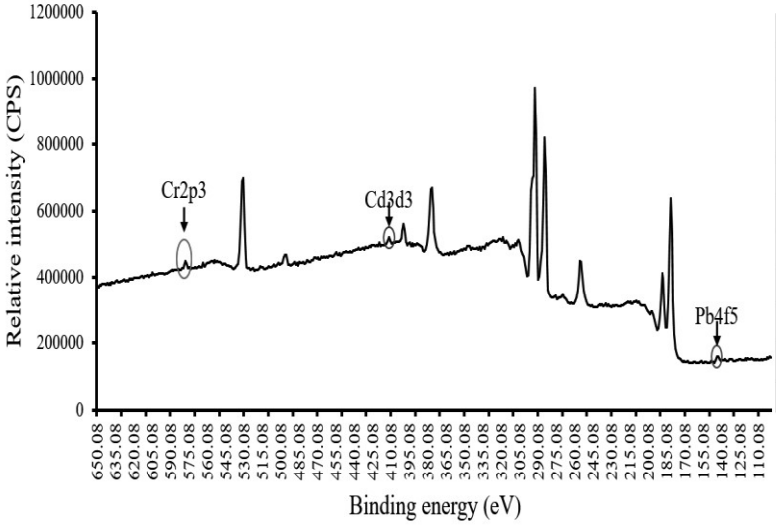

Name	Start BE	Peak BE	End BE	Atomic %
O1s	539.08	531.49	525.08	10.78
Na1s	1078.08	1071.21	1065.08	0.91
C1s	296	293.01	281	59.76
N1s	408	400.14	394	3.1
Cd3d3	417	412.13	410	0.02
Cd3d5	409	402.19	401	0.01
Cr2p3	579	577.91	575	0.03
Pb4f5	145	143.77	141	0.02
Pb4f7	140	137.92	136	0.01
Si2p	108	97.08	96	0.34

Figure 7.6 XPS spectra of *Microbacterium paraoxydans* strain VSVM IIT(BHU) after exposed simultaneous in ternary metal ion system of Cr (VI), Cd (II) and Pb (II).

The presence of heavy metals was observed in binding energy range of 579 to 575 eV, 417 to 410 eV and 145 to 141 eV for Cr2p3, Cd3d3 and Pb4f5, respectively. Similar results were also reported in the EDX analysis in the present study. Zhao et al., 2021 investigated Cd (II) removal by integration of sulphate reducing bacteria and zero valent iron. Authors reported binding of Cd (II) on the bacterial surface as Zn-S-Cd complex. Kim et al., 2021 performed XPS analysis of *Sporosarcina pasteurii* in the presence of divalent cations such as Cu, Zn, Pb, Cd and Sr in the bacterial growth medium. Authors reported the presence of divalent cations in the XPS analysis.

7.3.4 FTIR

FTIR analysis was performed to scrutinize the presence of functional groups on the bacterial surface. It also indicated changes in the function groups of the bacterial cell surface exposed to heavy metals. The FTIR spectra of control and heavy metal exposed bacteral cells are shown in the Figure 7.7.

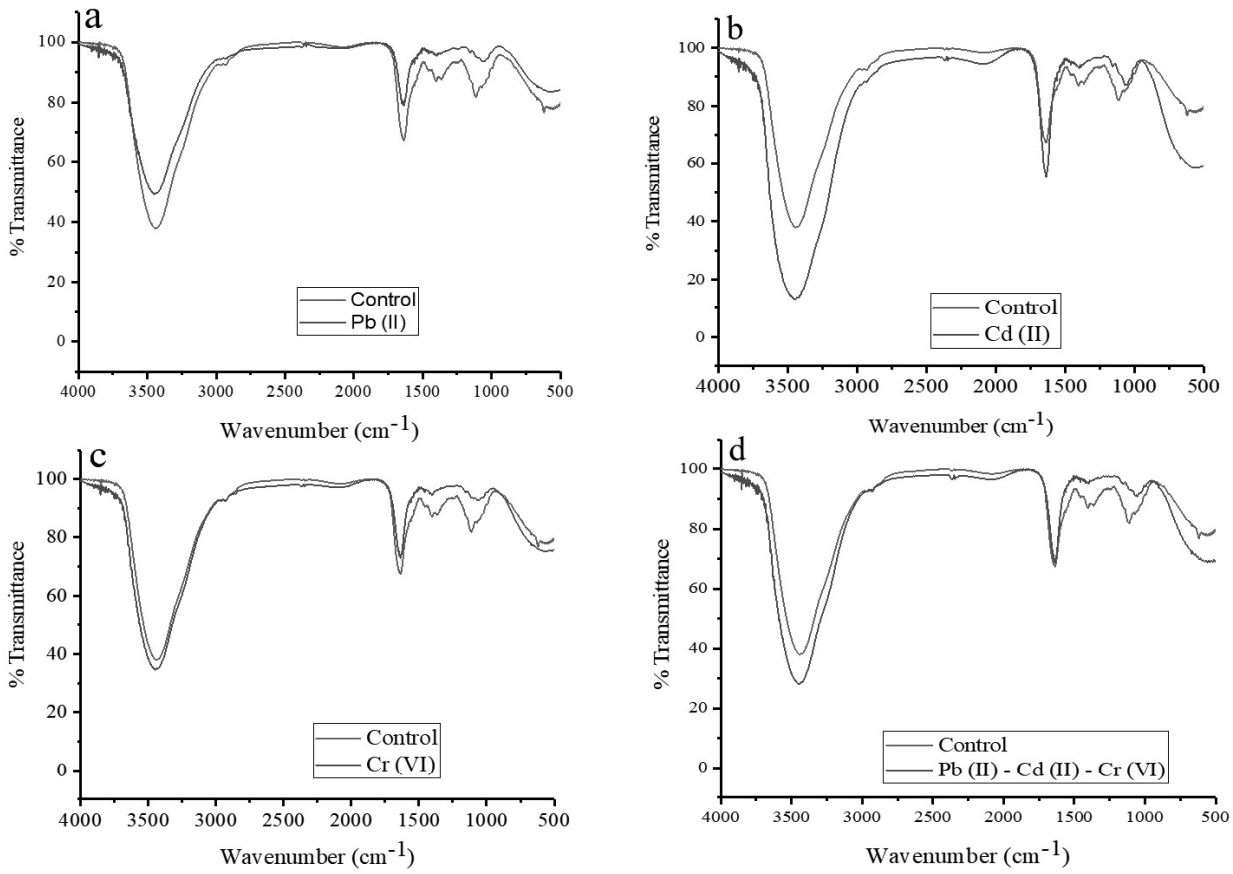

Figure 7.7 FTIR spectra of Pb (II) and control (**a**), Cd (II) and control (**b**), Cr (VI) and control (**c**), and ternary metal ions (**d**).

Transmittance peaks at 1,600-1,700 cm^{-1} indicated C=C groups, peaks at 1300-1400 cm^{-1} showed C-H stretching [Singh et al., 2020]. FTIR peaks at 1,050 -1,210 cm^{-1} reflected the presence of C-O and C-N groups of aliphatic compounds [Kibami et al., 2017; Saha et al., 2013]. FTIR spectra of the Pb (II), Cd (II), Cr (VI) and ternary metal indicated towards the shifting of FTIR spectra in the range of 1000-1400 cm^{-1} (Figure 7.7 a-d). Change in the FTIR spectra between 1300-1400 cm^{-1} indicated that C=C groups participated in binding of heavy metal ions. Shifting of the FTIR spectra at 1,050 -1,210 cm^{-1} indicated that C-O and C-N groups of bacterial cell surface were actively involved in the biosorption of heavy metal ions. Comparison of FTIR spectra of control and heavy metal exposed *Microbacterium paraoxydans* strain VSVM IIT(BHU) suggested that functional groups on the bacterial surface participated in the non-covalent and covalent interaction with heavy metal ions during biosorption [Singh

et al., 2020]. Wang et al., 2018 investigated Pb (II) biosorption mechanism in the *Arthrobactor* strain GQ-9. Authors performed FTIR analysis of bacterial cells and reported that hydroxyl, carboxyl, amino, nitrile and amide groups participated in the Pb (II) removal.

7.4.0 Effect of pH and temperature

The optimum pH is required for the activity of the several microbial enzymes involved in the cell growth. Another essential growth parameter is temperature which affects the growth of microorganisms. In the present investigation, *Microbacterium paraoxydans* strain VSVM was grown at various pH values **(**Figure 7.8a) and temperatures (Figure 7.8b).

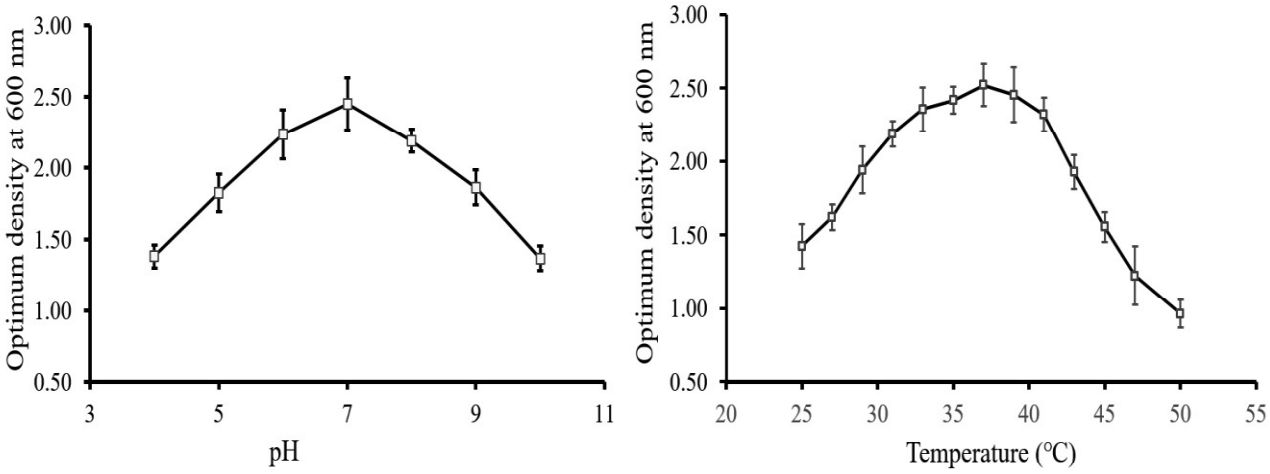

Figure 7.8 Effect of pH (**a**) and temperature (**b**) on the growth of the isolated *Microbacterium paraoxydans* strain VSVM IIT(BHU).

Figure 7.8a indicated that the bacterial growth was exponentially augmented with the increase in pH upto 7. The maximum growth was reported at pH 7 and decreased gradually above it. Growth rate of bacterial isolate increased with the rise in temperature up to 37ºC, which substantially reduced with the rise in temperature above it (Figure 7.8b). Maximum growth of *Microbacterium paraoxydans* strain VSVM IIT(BHU) was observed at pH 7 and 37°C in the LB broth. Sayyed et al., 2019 isolated *M. paraoxydans* from the dumping yard and maximum growth of the isolated bacteria was reported at pH 7. Laffineur et al., 2003 isolated *M. paraoxydans* sp. from a leukaemia patient and reported its maximum growth at 37ºC.

Buczolits et al., 2008 observed similar kind of results in the growth of *Microbacterium sp.* Elahi et al., 2019 isolated *Microbacterium testaceum* B-HS2 from tannery effluent and observed its maximum growth at pH 7 and 37°C.

7.5.0 Bacterial growth in presence of heavy metal ions and in control

The growth pattern of *Microbacterium paraoxydans* strain VSVM IIT(BHU) in the presence of single metal ions system such as Cr (VI), Cd (II), Pb (II), ternary metal ions and in control has been shown in Figure 7.9.

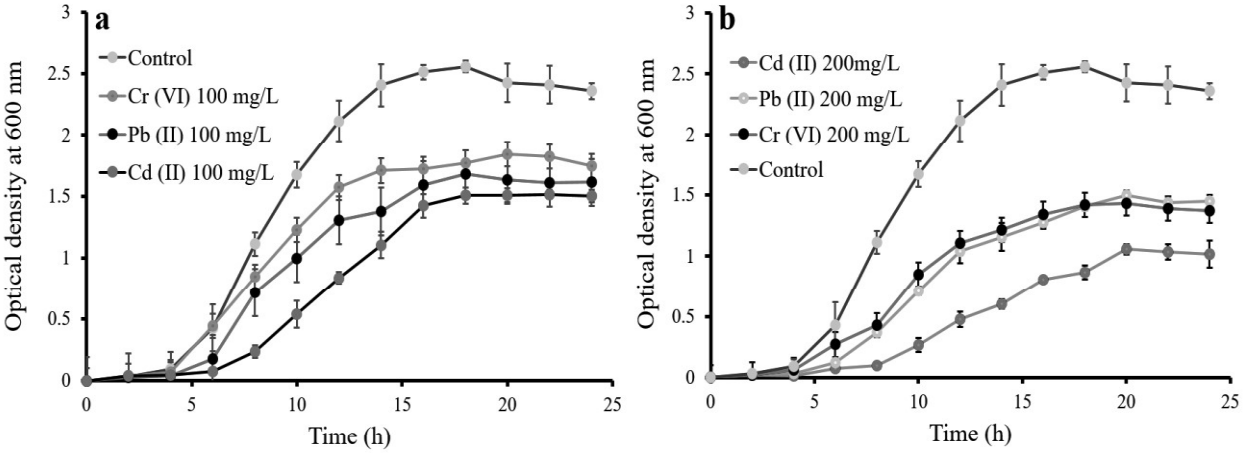

Figure 7.9 Effect of heavy metal on growth of *Microbacterium paraoxydans* strain VSVM IIT(BHU) at heavy metal concentration of 100 mg/L (**a**) and 200 mg/L (**b**).

It is evident from Figure 7.9 that the maximum growth of *Microbacterium paraoxydans* strain VSVM IIT(BHU) was in control. Cells grew well at 100 mg/L Cr (VI) (Figure 7.9a). However, the growth of *Microbacterium paraoxydans* strain VSVM IIT(BHU) in the heavy metal environment did not follow the similar growth rate as of control, which indicated heavy metal toxicity in the cells. The growth of bacterial strain was decreased when grown at heavy metal concentration of 200 mg/L. The similar growth pattern was observed when grown in 200 mg/L Cr (VI) and Pb (II), separately (Figure 7.9b). The minimum bacterial growth was reported at 200 mg/L Cd (II). No/ negligible growth of *Microbacterium paraoxydans* strain VSVM IIT(BHU) was observed above 300 mg/L.

The effect of Cr (VI), Cd (II) and Pb (II) on growth of *Microbacterium paraoxydans* strain VSVM IIT(BHU) was also observed in the ternary metal ion system. The effect of ternary metal system on bacterial growth was recorded at 50, 100, 150 and 200 mg/L of Cr (VI)-Cd (II)- Pb (II). The growth of *Microbacterium paraoxydans* strain VSVM IIT(BHU) in the presence of ternary metal system is shown in Figure 7.10.

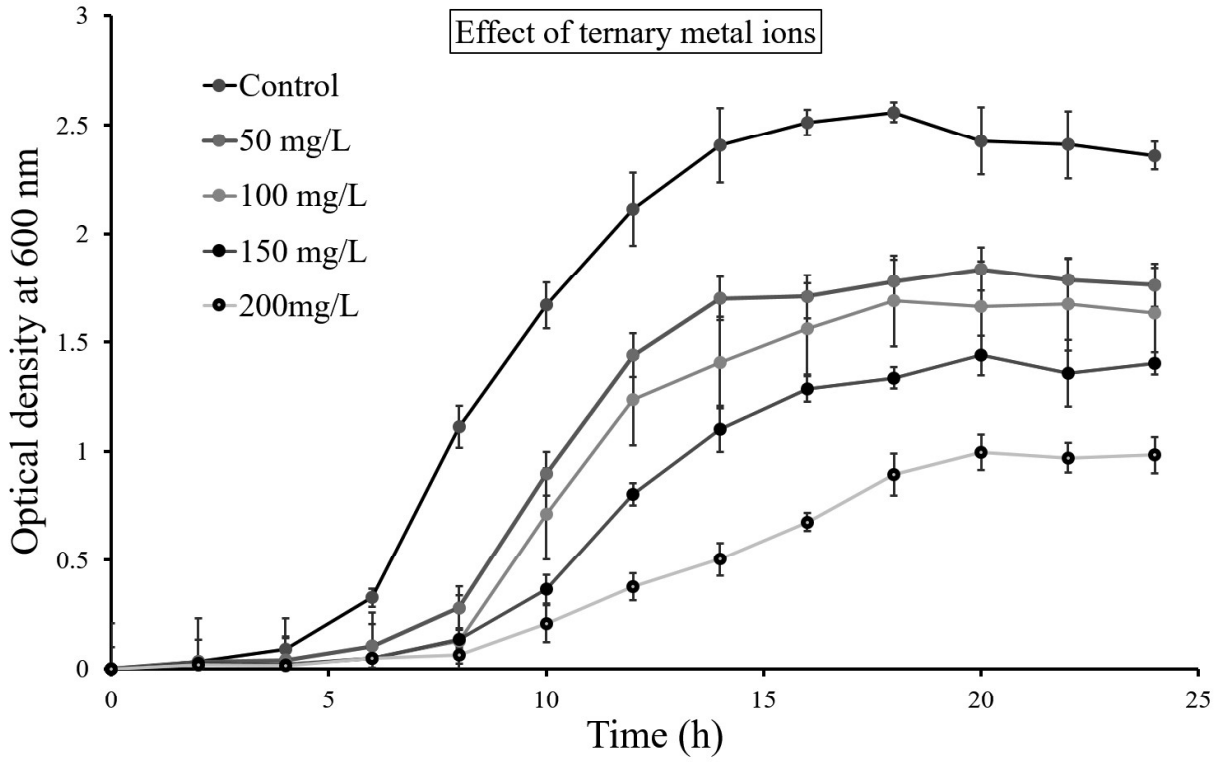

Figure 7.10 Effect of ternary heavy metal ions on bacterial growth

It became apparent from Figure 7.10 that maximum growth was reported in the control and minimum growth was reported in the 200 mg/L concentration of ternary metal ions complex. Maximum growth of *Microbacterium paraoxydans* strain VSVM IIT(BHU) was reported at 50 mg/L Cr (VI)-Pb (II)-Cd (II) after control. The growth of bacterial isolate decreased with rise in metal concentration due to its toxicity. The presence of heavy metals in the growth medium generates oxidative stress in the bacterial cell which inhibits the expression of several bacterial proteins including growth factors [Briffa et al., 2020].

Upadhyay et al., 2017 isolated *Bacillus* sp. MNU16 from soil contaminated with coal mining effluent. Authors evaluated the effect of Cr (VI) on the bacterial growth and reported that the growth rate reduced in the presence of Cr (VI). Nath et al., 2019 isolated *Bacillus megaterium* strain GCCSO1 from the contaminated soil sample. Bacterial isolate showed resistance against Cd (II), Pb (II), Cu (II) and Fe (II). Authors reported that *B. megaterium* strain GCCSO1 showed maximum growth in the presence of copper and lead and showed minimum growth in the incidence of cadmium. Masood and Malik, 2011 reported that the growth inhibition of *Bacillus* sp. FM1 was observed at 100 mg/L Cr (VI). Dey et al., 2014 isolated chromium resistant *Arthrobacter*, *Pseudomonas* and *Corynebacterium*. Authors reported that 50 % of bacterial growth decreased when bacteria was exposed to 2 mM Cr (VI). Dabir et al., 2019 isolated *Microbacterium oxydans* CM3 and *Rhodococcus* sp. AM1 from coal and aluminum mines. Authors estimated Cd (II) and Pb (II) removal efficiency of both bacterial isolates and reported that increase in concentration of Pb (II) and Cd (II) led to bacterial growth inhibition.

In the present work, the microbial cell viability was also estimated in term of CFUs/ml. The highest number of viable cells (9.5×10^5 CFUs/ml) were reported in control. Moderate cell count was observed in the 100 mg/L Cr (VI) (1.2×10^4 CFUs/ml), 100 mg/L Pb (II) (9.5×10^3 CFUs/ml) and 100 mg/L Cd (II) (6.3×10^3 CFUs/ml). The viable cells counts in the 200 mg/L Cr (VI) and 200 mg/L Pb (II) was reported 5.9×10^3 CFUs/ml and 2.9×10^3 CFUs/ml, respectively. The least viable cell counts were reported in the 200 mg/L Cd (II) (7.9×10^2 CFUs/ml).

The growth of bacterial isolate decreased due to heavy metal toxicity. Stress due to heavy metal ions was responsible for the ROS production, which increases significantly with the increase in concentration of heavy metal ions. ROS is responsible for the generation of oxidative stress in the cell which damages the cell organelles [Lazarova et al., 2014].

7.6.0 Heavy metal bioremediation mechanism

Heavy metal ions present in the aqueous solution cross the plasma membrane and enter into the intracellular space of bacterial cell. Passive diffusion is a simple mechanism in which small molecules cross the plasma membrane. The small molecules dissolve in the phospholipid bilayer and cross the plasma membrane and finally enter into intracellular space of the bacterial cell [Ma et al., 2009]. Intracellular heavy metal ions generate oxidative stress in bacterial cell which can damage the cell organelles. This heavy metal mediated stress can be neutralized by several antioxidant enzymes [Banerjee et al., 2015]. These antioxidants actively participate in the heavy metal bioremediation mechanism by bacteria. The heavy metal bioremediation mechanism can be decribed by heavy metal uptake dynamics and antioxidant system in the bacterial cell.

7.6.1 Expression of antioxidants

Toxic metal ions are responsible for generating the ROS, which disrupt cell organelles and are also responsible for the denaturation of nucleic acid and proteins within the cell [Ge et al. 2011]. The antioxidant enzymatic system minimizes the heavy metal toxicity within bacterial cell and makes them resistant to toxic metal up to a certain limit. In the present work, the stress marker activity (antioxidants) of catalase, SOD, GST and POX has been studied in *Microbacterium paraoxydans* strain VSVM IIT(BHU) exposed to heavy metal ions and in control (Figure 7.11).

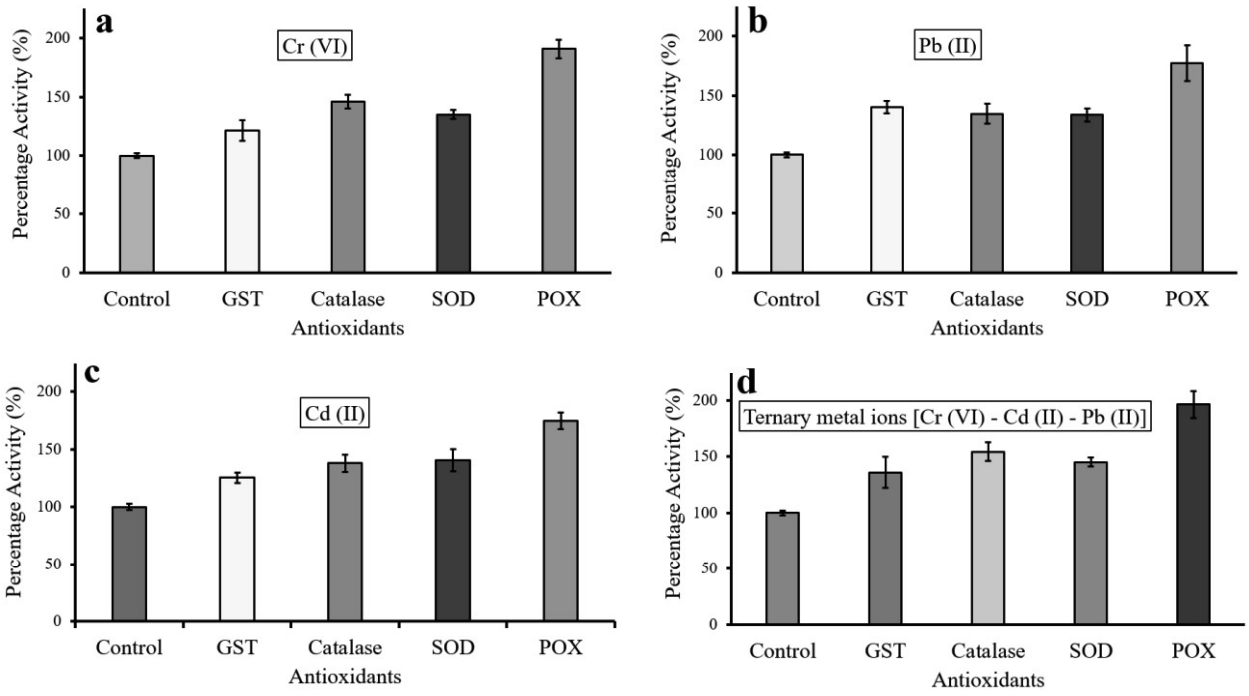

Figure 7.11 Antioxidant enzymatic activity in the *Microbacterium paraoxydans* strain VSVM IIT(BHU) grown in Cr (VI) (**a**), Pb (II) (**b**), Cd (II) (**c**) and ternary metal ions (**d**).

The antioxidant activity increased up to 21% (GST), 46% (catalase), 35% (SOD) and 90% (POX) in the Cr (VI) exposed *Microbacterium paraoxydans* strain VSVM IIT(BHU) as compared to control (Figure 7.11a). Likewise, the activity of GST, catalase, SOD, and POX enhanced up to 40.35 %, 34.49 %, 33.80 %, 77.32 % in *Microbacterium paraoxydans* strain VSVM IIT(BHU) exposed to Pb (II) (Figure 7.11b) as compared to control.

Similarly, the antioxidant activity in the Cd (II) exposed bacterial cell amplified up to 25.35 % (GST), 37.97 % (catalase), 40.25 % (SOD), and 74.67 % (POX) as compared to control (Figure 7.11c). The bacterial cells when grown in the medium containing ternary metal ions, it showed more expression of antioxidants in the microbial cells. The antioxidants expression in the bacterial cells enhanced up to 36.02 % (GST), 54.49 % (catalase), 45.13 % (SOD) and 96.32 % (POX) in presence of ternary metal ions (Figure 7.11d). The enhanced expression of antioxidants in the heavy metal exposed *Microbacterium paraoxydans* strain

VSVM IIT(BHU) indicated towards the bioaccumulation and toxicity of heavy metals in the intracellular space.

Lazarova et al., 2014 reported that the activity of SOD and catalase increased in *Trichosporon cutaneum* R57 when grown in the nutrient broth containing Cr, Pb and Cu. Similarly, Elahi et al., 2019 investigated the removal of Cr (VI) by *Microbacterium testaceum* B-HS2 and reported that the activity of antioxidants considerably increased due to Cr (VI) exposure. Hossan et al., 2020 isolated *Klebsiella* sp. from tannery effluent and reported that it was able to remove 95 % Cr (VI). Authors also observed the antioxidant profiling and reported that activity of antioxidant enzymes increased when the bacterial cells were grown in the Cr (VI) environment. Liao et al., 2020 investigated the Cr (VI) reduction and dynamic proteome response. Authors reported that GST and SOD played central role in Cr (VI) detoxification. Jobby et al., 2016 isolated *Enterobacter* sp. from the root nodules of *Sesbania sesban* and reported that antioxidants such as POX and CAT protect the intracellular organelles from ROS toxicity. Banerjee et al., 2015 isolated heavy metal resistant bacterial strain *Enterobacter cloacae* B1 from polluted soil and evaluated its heavy metal bioremediation efficiency. Authors reported that SOD activity was increased in the Cd (II) and Pb (II) exposed bacterial cells. The activity of catalase was also increased in the Cd (II) exposed bacterial cells. Steunou et al., 2020 explored the Cd (II) metal ion mediated stress in the bacterial cells. Authors observed that SOD activity in the bacterial cells increased when cells were exposed with Cd (II) containing growth media.

7.6.2 Heavy metal uptake dynamics

Passive diffusion is responsible for the majority of the uptake of several chemicals by bacteria, including Cr (VI), Cd (II), and Pb (II) ion [Kujawinski et al., 2000]. Passive diffusion is the simplest and unregulated technique of transporting a chemical across a membrane [Arnot et al., 2010]. When molecules are transported from one area to another, they follow a

concentration gradient, which is related to the transport of molecules from higher to lower concentration [Koul and Adlakha, 2021]. In order to explore the dynamics, the dimensionless numbers were explored in single and multi-metal solutions in this study. The dimensionless numbers are tabulated in the Table 7.2.

Table 7.2 Value of dimensionless numbers for metal ions in single and ternary metal ion system

Dimensionless numbers	φ	λ	N_k
Cr (VI)- single	1356.58	4.00×10^{-6}	9.09×10^{-3}
Cd (II) – single	1254.82	1.39×10^{-3}	9.83×10^{-3}
Pb (II) – single	1322.66	4.91×10^{-4}	9.32×10^{-3}
Cr (VI)-ternary	1300.00	8.03×10^{-4}	9.49×10^{-3}
Cd (II) –ternary	1243.15	1.54×10^{-3}	9.92×10^{-3}
Pb (II) –ternary	1001.90	3.86×10^{-3}	1.23×10^{-2}

In the present study, the value of N_k was observed between 10^{-3} and 10^{1} for all, which elucidated that heavy metal biosorption was mixed diffusion and transfer controlled. The value of φ and λ were in the range of 10^{-2} to 10^{4} and 10^{-12} to 10^{8}, which showed thorough coverage of bacterial surface during biosorption with reduced surface tension [Joos and Serrien, 1989; Ferri and Stebe, 2000].

7.7.0 Heavy metal removal efficiency of *Microbacterium paraoxydans* strain VSVM IIT(BHU)

The non-degradability and persistency of heavy metals make microbial bioremediation popular among researchers. Microbes consume trace amounts of heavy metals for their metabolic activities. However, they are tolerant/ resistant to higher concentration of heavy metal ions. The bioremediation of heavy metal ions by living cells is enzyme mediated, thus

pH and temperature play a crucial role in protein folding, enzymatic activity and ionization rate. This affects the uptake as well as intracellular detoxification of heavy metal ions [Zhang and Li, 2011]. The heavy metal ions removal is also dependent on contact time, initial metal ion concentration and optimum growth parameters (pH and Temperature) [Tang et al., 2021]. Singh and Mishra, 2021c studied the optimization pH and temperature for maximum bacterial growth. The authors reported that the maximum growth was at pH 7 and 37 °C. Thus, heavy metal removal by *Microbacterium paraoxydans* strain VSVM IIT(BHU) was performed at pH 7, 37°C and individually Cr (VI), Cd (II) and Pb (II) concentrations ranging from 50 to 200 mg/L and in ternary metal ion system (50 to 100 mg/L) (Figure 7.12).

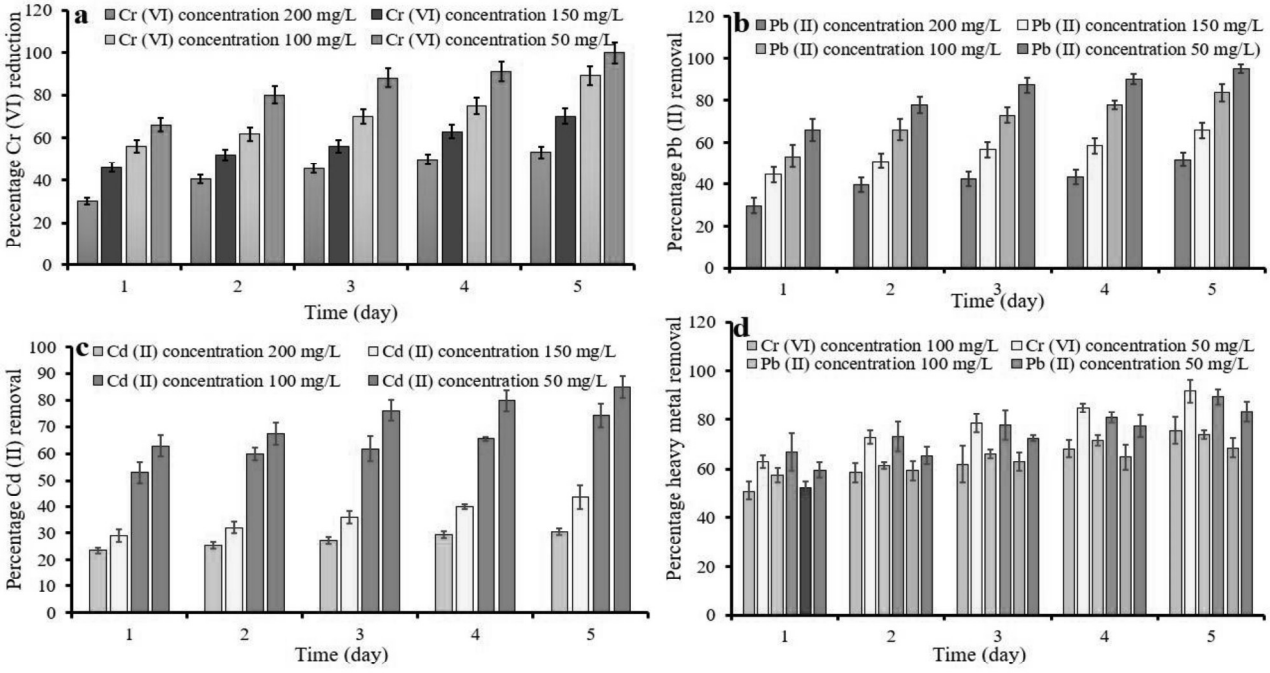

Figure 7.12 Heavy metal removal efficiency of *Microbacterium paraoxydans* strain VSVM IIT(BHU) in Cr (VI) (**a**), Pb (II) **(b**), Cd (II) (**c**) and ternary metal ion system of Cr (VI), Cd (II) and Pb (II) (**d**).

There was significant removal of Cr (VI) from the aqueous medium during the growth of *Microbacterium paraoxydans* strain VSVM IIT(BHU) (Figure 7.12a). The isolated strain removed 99.96 % Cr (VI) when grown in 50 mg/L Cr (VI) by 5th day. The removal of Cr (VI)

followed a similar pattern at all concentrations ranging from 50 to 200 mg/L. The minimum Cr (VI) (53.34%) removal was observed at 200 mg/L. The maximum (94.96%) removal of Pb (II) was observed at 50 mg/L and decreased with increase in Pb (II) concentration (minimum 52% removal was observed at 200 mg/L) (Figure 7.12b). Cd (II) also followed similar removal pattern to Cr (VI) and Pb (II). The maximum Cd (II) removal was observed as 84.96% at 50 mg/L Cd (II) and minimum (30.39%) removal was at 200 mg/L (Figure 7.12c). The metal removal efficiency was decreased when bacteria cells were grown in the ternary metal ion solution as compared to single metal ion solution (Figure 7.12d). Bacterial cells were grown in the 50 and 100 mg/L concentration of each metal ions. Cr (VI), Pb (II) and Cd (II) removal was reported as 91.62%, 89.29% and 83.29% at 50 mg/L, respectively. The removal efficiency decreased when *Microbacterium paraoxydans* strain VSVM IIT(BHU) was grown in 100 mg/L concentration in ternary metal ion system. Cr (VI), Pb (II) and Cd (II) removal efficiency at 100 mg/L was reported as 75.51%, 73.84% and 68.51%, respectively. In the present investigation, the bacteria mediated maximum removal of Cr (VI) and mimimum removal of Cd (II) was observed. *Microbacterium paraoxydans* strain VSVM IIT(BHU) followed the pattern as Cr (VI) > Pb (II) > Cd (II). The least removal of Cd (II) as compared to Cr (VI) and Pb (II) was might be due to its higher toxicity towards the bacterial cell which was also complemented with results shown in section 7.5.

Toxic heavy metals accumulate in the intracellular space of bacterial cell followed by their uptake in metabolic pathways. Heavy metals ions present in the growth medium aggregates on the bacterial surface and enters into the cell through various cell surface receptors and channels [Yilmazer and Saracoglu 2009]. Cr (VI) enters into the cell in the form of chromate through sulfate transporter due to its similar structure. The bacterial cell expels out excess Cr (VI) through their plasmid encoded ChrA protein [Malik 2004]. Intracellular Cr (VI) binds with metal binding proteins like metallothionein. The reactivity of $K_2Cr_2O_7$ is highly

dependent on the pH. Cr (VI) is less stable in an acidic medium in the form of $Cr_2O_7^{2-}$, while it is more stable in an alkaline medium in the form of CrO_4^{2-}. Cr (VI) can be easily transformed to Cr (III) in an alkaline medium [Stern et al., 2021]. The intracellular Cr (VI) reduction is mediated by enzymatic mechanisms and pH of the cell compartment. Reduced chromium gets bio-accumulated in the bacterial cell [Chojnacka 2010]. The heavy metals ions generate ROS stress in the bacterial cells. ROS mediated stress damages the protein and DNA of the bacteria. This ROS mediated stress can be neutralized through the high level activity of antioxidants like SOD, glutathione and catalase [Malik 2004].

Huang et al., 2001 investigated Cr (VI), Cd (II) and Pb (II) removal efficiency of *E. coli and B. subtilis* at 50 mg/L intial metal ions concentration. Authors reported that *E. coli and B. subtilis* was able to remove 63.39% and 69.90% Cd (II), 68.51% and 67.36% Pb (II), and 60.26% and 54.56% Cr (VI), respectively. Pal et al., 2005 isolated *Bacillus sphaericus* AND303 from serpentine soil of Andaman, India and investigated that isolated bacterial strain removed 72% Cr (VI) within 24 hours of incubation. Masood and Malik, 2011 isolated *Bacillus* sp. FM1 bacterial strain from the metal contaminated soil and the isolated strain removed 100 mg/L Cr(VI) in 48 hours. Panneerselvam et al., 2013 isolated a consortium of three bacterial species namely *Bacillus endophyticus*, *Microbacterium paraoxydans* and *Bacillus simplex*. The consortium was grown in Cr (VI) containing medium for three days and 92.6% removal was achieved. Su et al., 2018 investigated the Cr (VI) removal efficiency of photosynthetic bacterial isolates and reported that two out of all bacterial isolates showed 85 %Cr (VI) removal after 12 days of incubation. Dabir et al., 2019 isolated *Microbacterium oxydans* CM3 and *Rhodococcus* sp. AM1 from coal and aluminium mines. Authors recorded Pb (II) removal efficiency of *Microbacterium oxydans* CM3 and *Rhodococcus* sp. AM1 as 58 and 39% at 400 mg/L.

7.8.0 ANN Modeling

pH, contact time, and temperature were provided as network inputs, with the optical density of the sample being used as the target. In order to predict the output function, the feed-forward back-propagation network type was applied in conjunction with the Levenberg-Marquardt (L-M) algorithm. The network was trained until the lesser number of epochs were obtained. Thereafter, the experimental data was combined with the network simulation. The experimental findings were compared with predicted output function. The Mean Square Error (MSE) of the ANN model acquired in data training, testing, and validation is shown in Figures 13a-d for Cr (VI), Cd (II) and Pb (II) ions in single metal solution and ternary metal ions in multimetal solution, respectively.

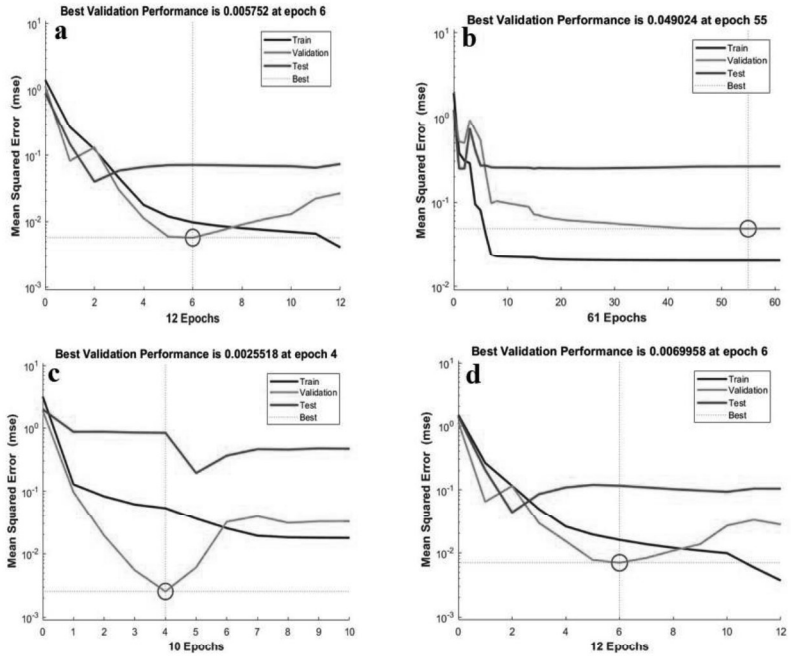

Figure 7.13 Performance between number of epochs and the MSE for Cr (VI) (**a**), Cd (II) (**b**), Pb (II) (**c**) ions in single metal system and ternary metal ion system (**d**).

During data training, testing, and validation, the L-M algorithm reported the lowest MSE (encircled point). Figures 7.14, 7.15, 7.16 and 7.17 show regression between experimental and predicted values for the adsorption of Cr (VI), Cd (II), Pb (II) ions in single

and ternary metal ion system. The circles in the plot are experimental values and the colored lines show the predicted values derived from ANN models. Both the experimental and theoretical values seemed to be in agreement with each other showing a high regression coefficient (R^2 value in range of 0.94 - 0.98) (Figure 7.14, 7.15, 7.16 and 7.17).

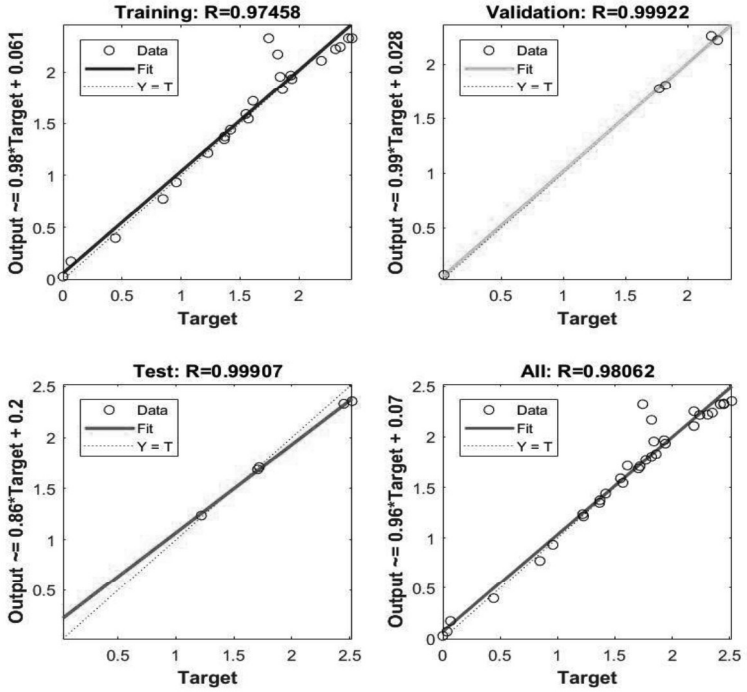

Figure 7.14 Regression plot for Cr (VI) ions in single ion system

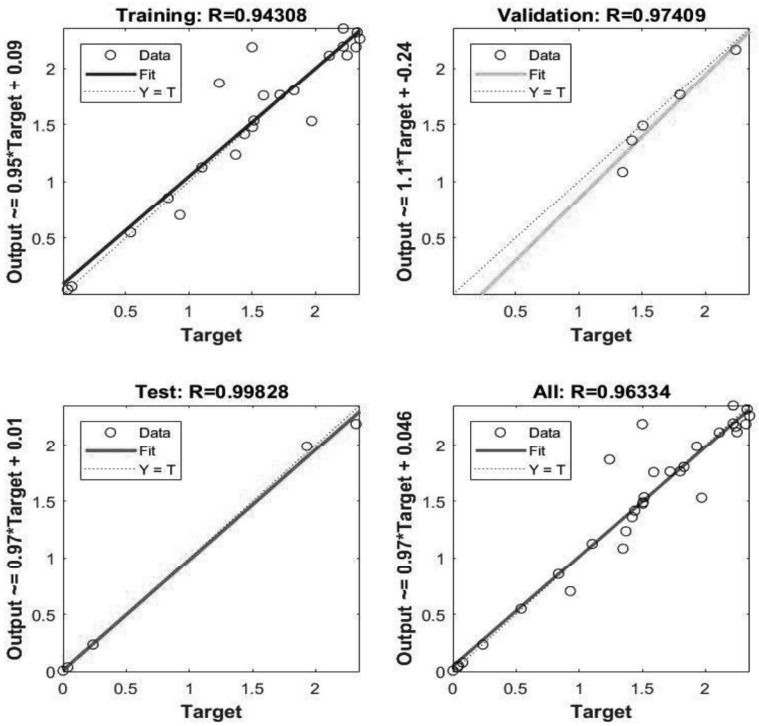

Figure 7.15 Regression plot for Cd (II) metal ion system

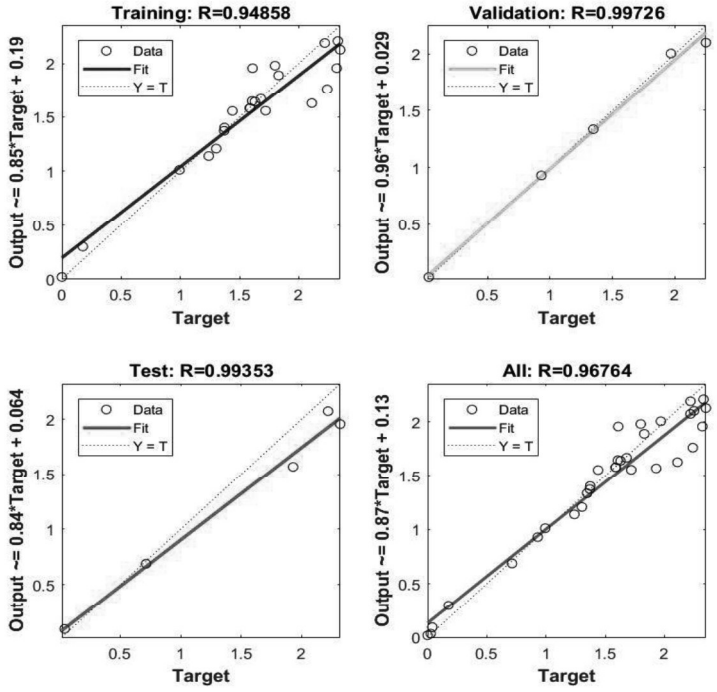

Figure 7.16 Regression plot for Pb (II) in single metal ion system

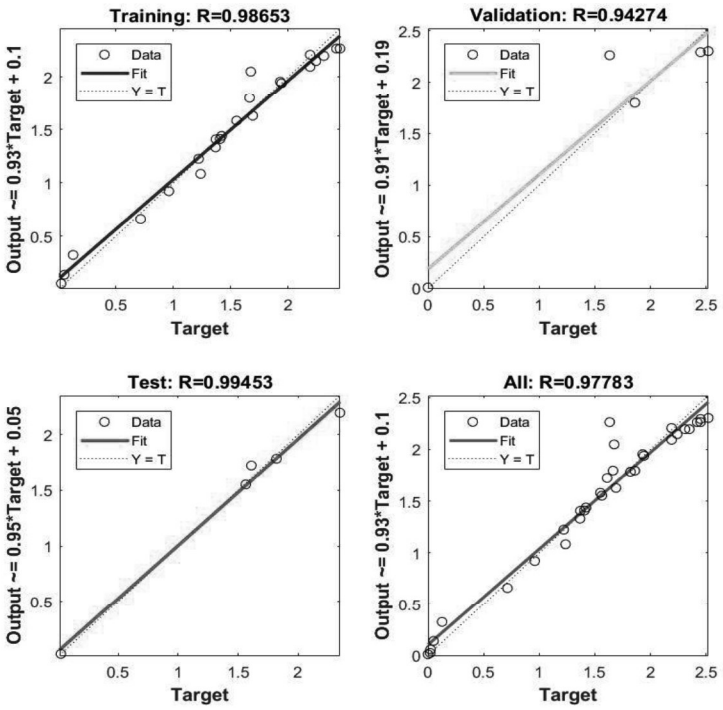

Figure 7.17. Regression plot for ternary metal ion system

Thus, in the present work, the L-M algorithm was concluded appropriate for predicting the output function with the lowest MSE at epoch (6, 55 and 4 for Cr (VI), Cd (II) and Pb (II) in single and 6 for ternary metal ion system) coupled with highest validation performance in ten neurons at 0.005752, 0.049024, 0.0025518 and 0.0069958 for Cr (VI), Cd (II), Pb (II) ions in single and ternary metal ion system, respectively.

The correlation plot showed high regression coefficient for Cr (VI), 0.050% for Cd (II), 0.063% for Pb (II) ions in single metal ion system and 0.003% for ternary metal ion system between the experimental and predicted values. The results also showed a small deviation of 0.012% for Cr (VI), 0.050% for Cd (II), 0.063% for Pb (II) ions in single and 0.003% for ternary metal ion system between the experimental and predicted values (Figure 7.18, 7.19, 7.20 and 7.21).

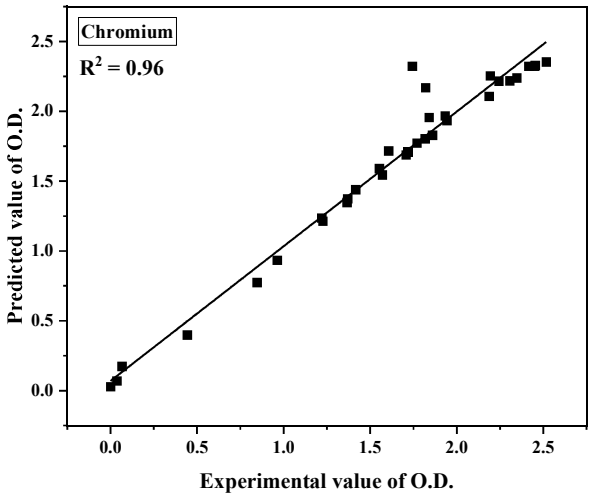

Figure 7.18 Correlation plot for the experimental and ANN predicted values for Cr (VI) ions in single metal ion system

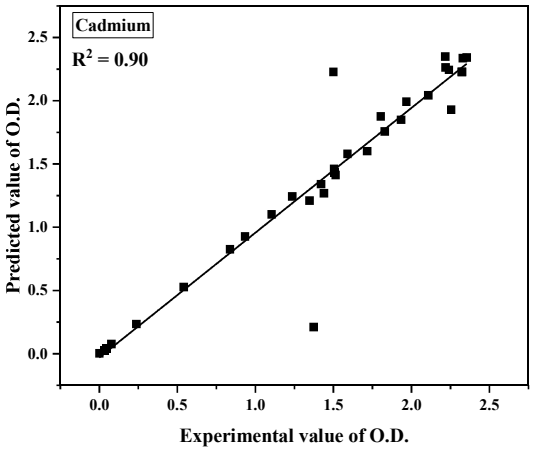

Figure 7.19 Correlation plot for the experimental and ANN predicted values for Cd (II) ions in single metal ion system

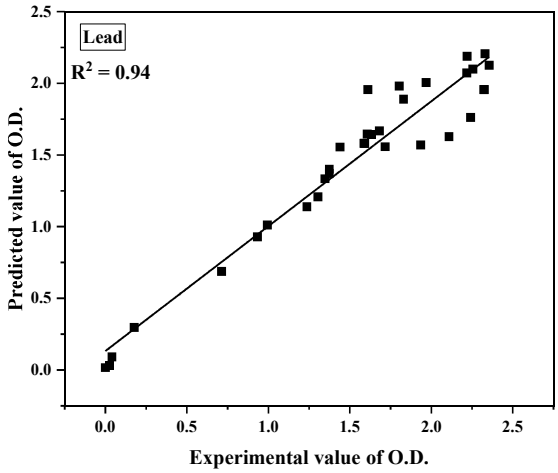

Figure 7.20 Correlation plot for the experimental and ANN predicted values for Pb (II) in single metal ion system

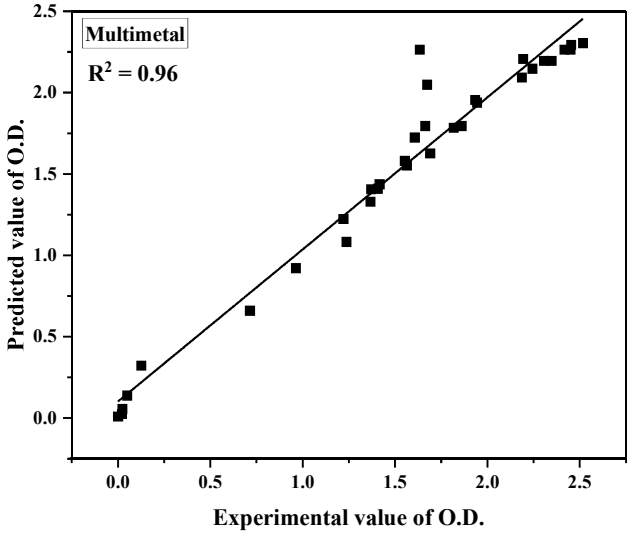

Figure 7.21 Correlation plot for the experimental and ANN predicted values for ternary metal ion system

This further showed the suitability of L-M algorithm in the present work. ANN modeling was used by Ghosh and Sinha 2015 to optimize the reduction of copper by *Stenotrophomonas maltophilia* PD2 BIOMASS and found R^2 of 0.958 from the trained network. Similarly, Talib et al., 2019 performed the optimization of chromium (VI) reduction

by newly identified *Acinetobacter radioresistens* strain NS-MIE from agricultural soil using ANN and found R^2 of 0.9991. Also, Ahmad et al., 2014 used ANN to predict the biosorption efficiency of immobilized *Bacillus subtilis* for removing cadmium ions and found R^2 of 0.997 between experimental data and model result. After performing ANN for modelling adsorption of Pb (II) from aqueous solution, Khan et al., 2017 obtained R^2 values in the range of 0.95 to 0.99 by experimenting with different functions.

7.9.0 Comparison of heavy metal removal efficiency

The comparative analysis of heavy metal removal efficiency of *Microbacterium paraoxydans* VSVM IIT(BHU) with other bacteria is shown in Table 7.3.

Table 7.3. Comparison of heavy metal removal efficiency

Bacterial species	**Heavy metal removal efficiency (%)**	**Initial Cr (VI) concentration (mg/L)**	**Incubation time (h)**	**References**
Cr (VI) removal efficiency				
Serratia sp. C8	80	20	120	[Gonzalez et al., 2014]
Enterobacter cloacae B2-DHA	81	1	120	[Rahman et al., 2015]
Ochrobactrum sp. YC211	96.5	30.2	32	[Chen et al., 2016]
Bacillus cereus strain NCr1a	73.7	10.4	72	[Tamindzija et al., 2019]
Bacillus cereus strain PCr12	74.4	10.4	72	[Tamindzija et al., 2019]
Enterobacter sp. SL	99.10	100	12	[Sun et al., 2020]

Acinetobacter radioresistens sp. NS-MIE	75.13	60	124	[Talib et al., 2019]
Bacillus cereus	96.85	50	48	[Zhao et al., 2012]
Microbacterium paraoxydans strain VSVM IIT(BHU)	99.96	50	120	Present study

Pb (II) removal efficiency

Urease-producing Strain Pb01	90	200	168	[Zhang et al., 2020d]
Phosphate-solubilizing bacteria Pb02	90	200	168	[Zhang et al., 2020d]
Bacillus sp.	99	100	--	[Gong and Li, 2011]
Achromobacter Sp. TL-3	80	1500	36	[Batta et al., 2013]
E. faecium Pb12	81.36	0.91	2	[Bhakta et al., 2012]

Microbacterium paraoxydans strain VSVM IIT(BHU)	94.96	50	120	Present study

Cd Removal efficiency

Microbacterium oxydans CM3	58	400	72	[Dabir et al., 2019]
Rhodococcus sp. AM1	39	400	72	[Dabir et al., 2019]
E. faecium Pb12	62.64	0.97	2	[Bhakta et al., 2012]
Pseudomonas sp. M3	70	100	24	[Abbas et al., 2014]
Burkholderia sp. strains ha-1	81.78	5 mM	24	[Yu et al., 2021]
Burkholderia sp. strains hj-2	79.37	5 mM	24	[Yu et al., 2021]
Burkholderia sp. strains ho-3	63.05	6 mM	24	[Yu et al., 2021]
Microbacterium paraoxydans strain VSVM IIT(BHU)	84.96	50	120	Present study

It is evident from Table 7.3 that extensive heavy metal removal potential exists in *Microbacterium paraoxydans* strain VSVM IIT (BHU). The high Cr (VI) removal efficiency

of *Microbacterium paraoxydans* strain VSVM IIT(BHU) is due to production of intracellular antioxidants, which makes this isolate more resistant against Cr (VI) and minimizes its toxicity.

7.10 Conclusion

Heavy metal resistant bacterial strain was isolated from coal mining wastewater and identified by 16S rRNA gene sequencing as *Microbacterium paraoxydans* strain VSVM IIT(BHU) MN650647. The optimum growth of *Microbacterium paraoxydans* strain VSVM IIT(BHU) was observed at pH 7 and temperature 37 ºC. The growth of bacterial isolate decreased with the increase in heavy metal concentration. GST, SOD, catalase and POX activities increased in the heavy metal exposed bacterial isolate which showed heavy metal toxicity and its bioaccumulation into intracellular space. The results of heavy metal removal dynamics of bacteria yielded by dimensionless numbers for Cr (VI), Cd (II), and Pb (II) ions revealed that heavy metal removal was regulated by mix diffusion and transfer process for both single and multi-metal ion system.

At lower heavy metal concentration, higher heavy metal removal efficiency was obtained by the bacterial isolate. SEM imaging showed the rod like and elongated structure of bacterial cells. FTIR analysis confirmed the presence of functional groups like C-H, C-O and C-N on the bacterial surface. The FTIR spectra change were in the range of 1300-1400 cm^{-1} and 1000-1300 cm^{-1}, corresponding to functional groups C=C and C-O, C-H, C-N on the bacterial cells exposed to the Cr (VI), Cd (II), Pb (II) of single and ternary metal ions system. Shift in the FTIR peak of bacterial culture after heavy metal exposure revealed successful bio sorption on the bacterial cell surface. XPS and EDX analysis both confirmed heavy binding with bacterial cells, and also indicated the presence of C, N, O in the bacterial culture which are important elements of bacterial cells. The surface carbon and oxygen rendered the *Microbacterium paraoxydans* strain VSVM IIT(BHU) a potential alternative for the biosorption of toxic heavy metal ions in the liquid phase. Heavy metal removal capacity of

bacterial decreased with rise in initial metal concentration and maximum removal was observed at 50 mg/L. The smallest MSE, 0.005752, 0.049024, 0.0025518, and 0.0069958, and the largest R^2 values, 0.98, 0.96, 0.97, and 0.98, were obtained with the L-M Algorithm for the prediction of optical density of Cr (VI), Cd (II), and Pb (II) ions in single and ternary metal ion system, respectively. The comparative study proved the *Microbacterium paraoxydans* strain VSVM IIT(BHU), a potential bacterial isolate for the removal of heavy metals from the liquid phase.